

Article

Assessing the Feasibility of Removing Graffiti from Railway Vehicles Using Ultra-Freezing Air Projection

Aina Vega-Bosch ^{1,*}, Virginia Santamarina-Campos ¹, Pilar Bosch-Roig ², Juan Antonio López-Carrillo ³, Vicente Dolz-Ruiz ³ and Mercedes Sánchez-Pons ²

¹ Department of Conservation and Restoration of Cultural Heritage, Faculty of Fine Arts, Polytechnic University of Valencia, 46022 Valencia, Spain; virsanca@upv.es

² Instituto Universitario de Restauración del Patrimonio, Universitat Politècnica de València, 46022 Valencia, Spain; mabosroi@upvnet.upv.es (P.B.-R.); mersanpo@crbc.upv.es (M.S.-P.)

³ CMT—Clean Mobility & Thermofluids, Universitat Politècnica de València, 46022 Valencia, Spain; jualoca6@mot.upv.es (J.A.L.-C.); vidolrui@mot.upv.es (V.D.-R.)

* Correspondence: aivebos@bbaa.upv.es; Tel.: +34-607919551

Featured Application: This study explores the viability of employing ultra-freezing air projection as a sustainable method to eliminate graffiti from rail vehicles and structures. Its potential application extends to the cleaning of non-porous materials, including industrial cultural heritage sites.

Abstract: Unauthorised graffiti is a challenge in urban environments, affecting railway structures, stations, tracks, and vehicles. Inefficient cleaning methods increase the costs and downtime of railcars, limiting passenger transport. In turn, they are harmful to the operator's health and the environment, due to the VOCs they release. This study focuses on the feasibility of dry-ice blasting, replacing carbon dioxide with ambient air as an innovative and sustainable solution to remove graffiti from rail vehicles. Experimental tests have been carried out with 13 different aerosols, controlling the temperature (<-80 °C), pressure (up to 3 bar), projection distance (0.5 cm) and exposure times (30"/1'/2'/4'/6'/8'/++). The results showed that ultra-freezing with ambient air preserved the integrity of the support materials and altered the topography, colourimetry and adhesion of the aerosols tested, achieving the total removal of one of the paints. Preliminary results suggest that ultra-freezing with ambient air could be a viable and sustainable solution for graffiti removal on railway structures, transferable to other urban environments.

Keywords: ultra-cold air jets; cryogenics; eco-sustainable gases; environmental sustainability; environmental impact; aerosol adhesion; cleaning innovation; graffiti removal; aerosol sprays; eco-friendly gas

Citation: Vega-Bosch, A.; Santamarina-Campos, V.; Bosch-Roig, P.; López-Carrillo, J.A.; Dolz-Ruiz, V.; Sánchez-Pons, M. Assessing the Feasibility of Removing Graffiti from Railway Vehicles Using Ultra-Freezing Air Projection. *Appl. Sci.* **2024**, *14*, 4165. <https://doi.org/10.3390/app14104165>

Academic Editor: Giuseppe Lazzara

Received: 11 April 2024

Revised: 11 May 2024

Accepted: 11 May 2024

Published: 14 May 2024



Copyright: © 2024 by the authors. Licensee MDPI, Basel, Switzerland. This article is an open access article distributed under the terms and conditions of the Creative Commons Attribution (CC BY) license (<https://creativecommons.org/licenses/by/4.0/>).

1. Introduction

Unauthorised graffiti is one of the most significant issues in urban environments. It affects any accessible surface, driven by the recognition and the sense of publicity that some media can provide for the author and their message [1,2]. Nowadays, recognition is reinforced through images uploaded to the Internet after the original is removed, promoting in turn the areas in which they were made [3]. These types of actions are mainly found in cities, affecting road structures and environments such as bridges, acoustic walls, retaining walls and traffic signs [4]; on the façades of buildings, such as schools, private residences, train stations, means of transport and street furniture [5]; as well as on protected urban vegetation such as monumental trees [6]. Some authors theorise that illicit graffiti can generate environments where the 'broken windows' phenomenon occurs, whereby if one window in a building is broken and not quickly

repaired, other windows will also be broken [7]. They argue that this phenomenon perpetuates the perception of institutional neglect and lack of interest, which in turn can encourage other types of crime or reoffending [8]. Other perspectives consider graffiti and street art as forms of communicative political participation, relating them to social criticism in cities [9]. From this position, preventive solutions are proposed for the management of graffiti in cities, favouring coexistence among communities. Examples of this are Vienna (Austria), Berlin (Germany) [10] and Sydney (Australia) [11], where specific legal zones for the use of aerosols are being designated to reduce unauthorised interventions on public and private property. This measure seeks to control and regulate graffiti by providing a designated space for it and minimising its presence elsewhere in the city.

From the above, it can be stated that street graffiti generates social, political, and economic conflicts, as well as environmental struggles due to the release of volatile organic compounds present in the spray cans [12]. Clean-up as an option for sustainable solutions is an important economic cost for both public and private entities. Aerosol disposal amounts to USD 12 billion per year in the US and GBP 100 million per year in the UK [13]. In Spain, graffiti removal from buildings in Madrid costs up to EUR 10,000 per day, and since 2017 these cleaning actions have increased by 81% [14].

In transport, illicit graffiti is the most common form of vandalism, referring to the rail network and related infrastructure, and is responsible for a large proportion of incidents [15]. It represents a public safety problem because of the risks to which the perpetrators of graffiti on tracks and in tunnels are exposed, while there are economic and operational costs associated with the repair and removal of the graffiti [16]. Train cars, sidings and stations can be considered state property and their damage can be interpreted as a means of making anti-government and/or political statements [3]. However, they may be considered visible property damage and some investigators claim that they impact passenger flow by being perceived as features indicative of risk, insecurity and neglect [17]. According to Enever (2013), graffiti is challenging for railway operators. In addition to the costs associated with repairing or replacing vandalised rolling stock, there is a considerable cost associated with cleaning trains, stations and other rail infrastructure affected by graffiti. It states that there are increased safety risks, such as damage to signals, which can lead to dangerous situations, such as derailments, and these incidents can result in delays or cancellations of services. All these factors contribute to the increased operational and legal costs associated with dealing with vandalism and graffiti in the rail sector. [18].

The economic impact of graffiti interventions on trains extends to all cities around the world. The magnitude of the associated costs is not only linked to the number of cases, but also to the strategies implemented for prevention and clean-up. Taking the Spanish transport operator Renfe as an example, in 2018, it spent EUR 15 million on cleaning up its fleet, removing 4000 graffiti acts [19], equivalent to the purchase of three trains [20]. However, by 2020, the costs amounted to EUR 25 m [20], marking an increase of 166%. Catalonia (the autonomous Spanish community) incurred expenses of EUR 6.5 million in 2021 alone to combat graffiti, affecting almost 80% of the trains in circulation. [21]. The persistence of the problem led Renfe to normalize, in 2023, a large contract of almost EUR 40 million for the provision of graffiti removal and cleaning services [22]. This situation is not unique to Spain, as other countries such as Belgium, the Netherlands, Germany and Australia also face similar challenges. Brussels, the capital of Belgium, allocated EUR 4.2 million in 2018 to remove graffiti from its train fleet, a figure that increased to EUR 6.15 million in 2020 [23]. In the Netherlands, spray interventions represent an annual investment of EUR 10 million. In Berlin, the capital of Germany, EUR 10 million is spent annually, according to the BVG Berlin [24]. In Australia, Sydney Trains New South Wales faces an annual expenditure of EUR 30 million to remove graffiti from its rail fleet [25]. This situation reflects a common challenge faced by rail authorities around the world.

One of the main problems we identified is linked to the method of cleaning. Currently, the main methods of graffiti removal in the railway industry are mechanical removal (brushes, scrapers, and scouring pads) and chemical cleaning (solvent mixtures of hydrocarbons, ethers and/or alkalis). They are sometimes combined or complemented to ensure satisfactory recovery of trains. Generally, the remover is applied by spraying or depositing it with a brush. It is left to act for the time stipulated by the manufacturer. It is then removed by abrasive methods such as brushes or pressure jets and cleaned one last time with soap and water. Finally, a hot water rinse is applied to the entire carriage [26]. However, chemical removal methods may yield unsatisfactory results, requiring repainting or re-stripping of the convoys. According to some authors, this problem may be aggravated by the colour of certain aerosols, such as red and blue, which are difficult to remove, causing losses and unsatisfactory results, making it necessary to propose another type of treatment [27].

In addition, the effect on the health of operators using the chemical methods traditionally used for the removal of graffiti on railway supports has been studied [28]. They were declared as potentially toxic and irritating to the skin, eyes and mucous membranes [29]. The harmful effects on the health of workers related to the chemical composition of the solvent mixtures are as follows [10,28,29]:

- Ethylene glycol ethers: May affect reproductive functions and the respiratory system. Penetrate through the skin.
- Limonene: May cause eye irritation and alteration of the respiratory tract. Dermal disorders.
- Methyl ethyl ketone (MEK): may cause headaches, eye irritation, respiratory impairment and may impair cognitive functions, e.g., causing a loss of balance.
- Methylene chloride: This is an irritant carcinogen that may cause eye irritation, impaired respiratory tract and cognitive functions, such as loss of balance. Prolonged exposure may cause liver and kidney damage or changes in the blood's ability to carry oxygen.
- N-methylpyrrolidone (NMP): This is a carcinogen that may affect reproductive functions. Skin effects are swelling, blistering and burning.
- Toluene: This is an irritant to the eyes, respiratory system and dermis. May cause headaches and cognitive impairment.

There is also an environmental impact of these solvents. Alcohols and hydrocarbons, such as N-methylpyrrolidone (NMP) [10] traditionally used in train cleaning, have high concentrations of Volatile Organic Compounds (VOCs), the main risk of which is atmospheric pollution, measured as the Global Warming Potential (GWP) and Ozone Depletion Potential (ODP) of each component. The most common alkalis include sodium hydroxide, better known as caustic soda, and potassium hydroxide. Dissolving sodium hydroxide and potassium hydroxide in water produces a strong base that reacts dangerously with acids, and its coming into contact with the environment should be avoided by all means [30]. Thus, inadequate waste management resulting from the use of these products can contribute to acute wastewater pollution, severely altering the marine ecosystem.

Within the conception of graffiti as an intolerable act of vandalism, measures have been taken to combat it and prevent its spread in cities [8,31,32]. Some authors advocate that it should be cleaned up in the shortest possible time to discourage other graffiti artists from intervening in the same area [33]. Thus, they propose increasing the control and criminalisation of these acts, while maintaining traditional clean-up methods. Other solutions have aimed at simplifying and speeding up the cleaning process, by studying "sacrificial" or permanent anti-graffiti products as intermediate layers between the surface and the aerosol, thus facilitating the cleaning of surfaces [34,35]. Semi-permanent or "sacrificial" coatings, usually wax, are removed during the cleaning process, usually with hot water, while permanent coatings are designed to withstand frequent and repeated

cleaning cycles and are the preferred choice for trains [36]. The benefits of this are the reduction in cleaning time in the railway sector, allowing the quick return of the car to the line, although the abuse of water resources may be a problem in the medium-to-short term. In this respect, cleaning products are also being designed using environmentally friendly solvents, reducing the harmfulness to the operator [37].

Given the complexity of the challenge, there was a call for technological innovation in Ireland. A call for innovative solutions in the process of cleaning graffiti from rail transport was formalised. Irish Rail proposed an investment of EUR 150,000 to introduce innovative proposals to reduce the financial outlay for this type of treatment [38]. In Spain, the Spanish national railway company (Renfe) also wanted to promote an innovative proposal through a campaign to raise public awareness of the cost of removing graffiti from its train fleet. The strategy consisted of integrating an aerosol-painted train door among the artworks at the Madrid International Contemporary Art Fair (ARCO). They published a photograph on social networks, with the caption 'This train door is #LaObraMásCara de #ARCO2019, worth EUR 15 million. And we all paid for it' [39]. However, the costs incurred by the company the following year (2020) showed an increase in the budget for graffiti removal of 166%, a total of 68,000 square meters of surface area [40]. Following this campaign, it was confirmed that the way to reduce the amount of money spent on ink and spray removal required a change of strategy and a focus on minimising working times, i.e., improving the efficiency of the cleaning method.

The disadvantages of the current cleaning processes are directly related to efficiency, and with unsatisfactory removal: the economic cost related to the working hours of the cleaning operators, the safety of the treatment due to the high toxicity of the solvents, and environmental pollution, involving a high risk to the marine ecosystem, the emission of greenhouse gases and a high consumption of water resources. On the other hand, it can also be stated that they are cleaning methods that damage the underlying materials, affecting the vehicle's finish and supports, and forcing the extension of a train's stoppage times, which disrupts timetables and passenger transport.

Research in other industrial and heritage sectors has focused on exploring new cleaning systems that minimise working times and toxicity and improve efficiency [41]. These include cryogenic CO₂ 'dry-ice blasting' by projection of solid CO₂ in pellet form [42], or 'snow blasting' liquid CO₂ in mist form [43]. This technique was initially developed as a degreasing method and has evolved significantly since its introduction onto the market in the 1980s. It provides an innovative approach to surface cleaning, its effectiveness being based on three mechanisms: thermal shock through cooling, kinetic energy generated by compressed air and impact, and sublimation of the projectile [44].

The advantages of this system over other cleaning methods have been studied. Firstly, it provides an eco-sustainable approach by projecting recycled CO₂, which reduces water consumption and eliminates the need for solvents that damage the environment and health [45]. In addition, it ensures the safety of the surfaces by avoiding abrasion due to the low hardness of the pellets used (2 Mohs) [46] and favours the reduction in air pressure required compared to other mechanical methods [47]. It is a versatile cleaning method, due to its ability to adapt to different parameters and delicate surfaces [48] and unique treatment, as it does not leave residues on the treated surface that would require a second washing or drying of the surface [49]. On the other hand, a comparative study with other types of spraying methods such as sand blasting or water blasting, carried out by researchers from the Department of Civil, Architectural, and Environmental Engineering of the University of Miami, found that it required 19% less energy than other techniques, in addition to reducing the average time of use by 77%, validating it as an efficient and safe technique for its application to architectural structures [50]. However, due to the nature of the projectile, CO₂ cleaning recorded the highest values of greenhouse gas emissions. Although dry-ice blasting favours the reuse of surpluses and by-products, the production of this material being an inherent process in the manufacture of other gases such

as oxygen, argon and hydrogen [51], reducing the release of carbon dioxide into the atmosphere is a new challenge in cryogenic studies.

In the search for solutions, a collaboration between research departments arose for the adaptation of equipment designed to carry out refrigeration cycles at temperatures below -150 °C [52–54]. This is an installation whose innovation lies in the use of ambient air as the refrigerant fluid, avoiding the environmental and economic impact of the use of cooling liquids, since air (known as a refrigerant with the code R-729) has null ODP and GWP, is plentiful and has no cost, and is harmless, non-flammable, non-reactive, and, of course, breathable, avoiding any impact on the health of the workers that employ this technology. The technology has been adapted and transferred to the medical (vaccine preservation), automotive (ultra-fast battery charging) and agri-food (food preservation) industries. Figure 1 illustrates the experimental installation designed to produce low-temperature air jets. The configuration used in the installation corresponds to a reverse Brayton cycle, comprising three consecutive stages of air compression.

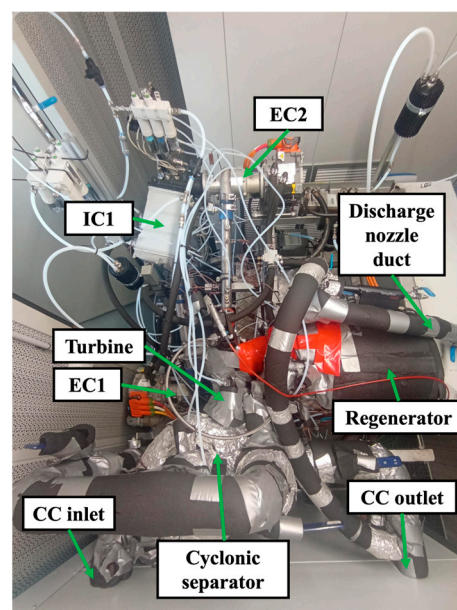


Figure 1. Installation of the reverse Brayton cycle (RBC). Source: own elaboration, 2023.

The first two compression stages are electrically driven (stages 1–2 and 3–4 in Figure 2), while the third stage is driven by the compressor of a turbocharger (stage 4–5). The latter uses the energy of the turbine to generate additional pressure in the air. Between the compression stages there are two heat exchangers (stages 2–3 and 5–6) in which the air, previously heated by the compression processes, is cooled using water at ambient temperature. After the compression stages, there is a regenerative phase prior to the expansion (stage 6–7), which makes it possible to take advantage of the part of the cycle in which the air is at low temperature and pressure to continue cooling it to below ambient temperature. After the regenerator, the air enters the turbine and expands until it reaches its minimum temperature in the cycle, which can be as low as -180 °C . After the turbine, the cold air is used to cool the thermal load (stage 8–9). Once the thermal load has passed, the air, still at low pressure and below ambient temperature, returns to the regenerator (stage 9–1) to cool the regenerated air before it enters the turbine. On leaving the regenerator, the air is directed back to the first compression stage, closing the loop of the cycle.

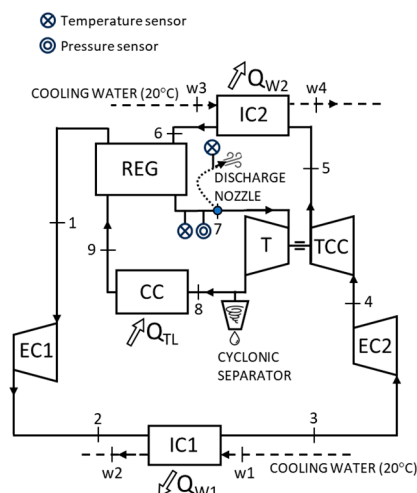


Figure 2. Scheme of operation of the cycle. Source: own elaboration, 2023.

For the current application, where it is required to generate air jets with high velocities and low temperatures, a partial air extraction is performed at point 7 of the scheme shown in Figure 2. At this point, the air has a high pressure and temperatures below ambient temperature (with values close to $-80\text{ }^{\circ}\text{C}$). To achieve high velocities in the air jet and maintain low temperatures, this air is expanded through a nozzle and released into the environment. The air extraction is carried out by means of a flexible hose that connects the air outlet point, where the extraction occurs, through a convergent–divergent nozzle. Two of the nozzles designed for extraction can be seen in Figure 3. Different nozzle geometries were 3D printed to vary the mass flow ratio ejected.



Figure 3. Discharge nozzles. Source: own elaboration, 2023.

The objectives of this research are as follows:

1. To evaluate the low-temperature resistance of materials used in transport vehicles through experimental laboratory tests.
2. To adapt the deep-freezing equipment for experimental tests in the laboratory.
3. To analyse and discuss the data obtained in the experimental tests, assessing the feasibility of the project of using deep-freezing equipment for removing graffiti from railway vehicles. This will consider technical, economic, and environmental aspects, and propose improvements and solutions to the problems identified.

Research on green technologies implementable in various sectors also contributes to the 2030 Agenda (SDG3; SDG7; SDG8; SDG9; SDG12; SDG13) and its pact with environmental protection, as well as to the recommendations of the 2030 Agenda for Change, by contributing to the industrial transition.

2. Materials and Methods

2.1. Support and Selected Graffiti

The experimental study was carried out on a substrate with the usual red metallic-paint coating, referred to in the study as COA1. Thirteen different aerosols were applied (Table 1), distributed in a grid over the surface. The choice of the aerosols tested was based

on their usual presence in graffiti environments. The most representative and complex colours are the most researched in environments dedicated to the conservation of urban art [55], for which we have more information regarding their composition, mechanical behaviour, and degradative response to extrinsic and intrinsic agents of the material [56].

Table 1. Physical and chemical characteristics of the materials applied on the COA1 specimen. Source: own elaboration based on manufacturer’s data sheets [57–61].

Code	Manufacturer	Type	Colour	Gloss ^{60°}	Dry Film Thickness	Accession	Medium	Solvent	Opacity	UV Resistance
1_MTN_94_R 2_MTN_94_R	MTN	MTN 94	RV 3001 Vivid Red EX014H3001	15–25% matte	15–20 µ/layer	0 B	Modified Alkyd	Aromatic mixture	5 of 5	2 of 3
3_MTN_WB_R 4_MTN_WB_R	MTN	Water-based	NAPHTHOL RED—PW6- PR170-PO34-PY74-PY42 RV 3020 Light Red EX019W3020M	<10% matte	15–20 µ/layer	0 B	Modified Polyurethane	Water and alcohols	4 of 5	2 of 3
5_MTN_94_V 6_MTN_94_V	MTN	MTN 94	RV 6018 Valley Green EX014H6018	15–25% matte	15–20 µ/layer	0 B	Modified Alkyd	Aromatic mixture	5 of 5	3 of 3
7_MTN_WB_V 8_MTN_WB_V	MTN	Water-based	BRILLIANT GREEN—PW6- PY74-PG7-PR122 RV 6018 Valley Green EX019W6018M	<10% matte	15–20 µ/layer	0 B	Modified Polyurethane	Water and alcohols	5 of 5	2 of 3
9_MTN_94_A 10_MTN_94_A	MTN	MTN 94	RV 30 Electric Blue EX014H0030	15–25% matte	15–20 µ/layer	0 B	Modified Alkyd	Aromatic mixture	5 of 5	3 of 3
11_MTN_WB_A 12_MTN_WB_A	MTN	Water-based	COBALT BLUE—PW6- PB153-PB29-PY74-PR122 RV 68 Hope Blue EX019W0068M	<10% matte	15–20 µ/layer	0 B	Modified Polyurethane	Water and alcohols	5 of 5	3 of 3
13_MTN_94_M 14_MTN_94_M	MTN	MTN 94	RV 175 Electra Violet EX0140175MRV	15–25% matte	15–20 µ/layer	0 B	Modified Alkyd	Aromatic mixture	5 of 5	3 of 3
15_MTN_WB_P 16_MTN_WB_P	MTN	Water-based	DIOXAZINE PURPLE— PW6-PV23-PBK7-PG7-PB153 RV 173 Ultraviolet EX019W0173M	<10% matte	15–20 µ/layer	0 B	Modified Polyurethane	Water and alcohols	5 of 5	3 of 3
17_MTN_94_N 18_MTN_94_N	MTN	MTN 94	Matte Black EX014H0901	15–25% matte	15–20 µ/layer	0 B	Modified Alkyd	Aromatic mixture	5 of 5	3 of 3
19_MTN_WB_N 20_MTN_WB_N	MTN	Water-based	CARBON BLACK—PBK7 R 9011 Black EX019W9011M	<10% matte	15–20 µ/layer	0 B	Modified Polyurethane	Water and alcohols	5 of 5	3 of 3
21_MTN_N2G_N 22_MTN_N2G_N	MTN	NITRO 2G	NITRO 2G Black. Solid colour. Matte Paint.	<10%	20 µ/layer	3 B	Acrylic	Butyl Acetate	5 of 5	3 of 3
23_MTN_T 24_MTN_T	Montana	Tarblack	Black Tarblack	Matte	-	-	Bitumen-base	-	5 of 5	3 of 3
25_MTN_HP 26_MTN_HP	MTN	Hardcore	Silver EX014H0101	60–85% glossy <20% matte	15–20 µ/layer	0 B	Modified Alkyd	Aromatic mixture	5 of 5	1 of 3
27_PC5M_N	POSCA	Marker PC5M	Black	-	-	-	-	Water and alcohols	5 of 5	3 of 3

The application of the materials was carried out under standard environmental conditions, following the manufacturer’s instructions for application, drying and handling. The tests were carried out after three months of drying. Each colour sample was confined to 10 × 10 cm areas, grouped by colouring substances and binders (Figure 4). There was a 2 mm overlap with the adjacent colours and a 2.5 mm POSCA marker line was drawn over each aerosol, generating a grid pattern, reiterated in all quadrants as illustrated in the 27_PS5M_N matrix (Figure 4).



Figure 4. Aerosol distribution scheme. Source: own elaboration, 2023.

Physical and Chemical Characteristics of the Aerosols

The physical and chemical characteristics of the products tested in sample COA1 were defined according to the safety data sheets and data sheets provided by the manufacturers. [57–61]. Aerosols with different binders were selected: modified alkyd, modified polyurethane and bituminous base. These binders are diluted in hydroalcoholic solvents or aromatic diluents, which influence the formation of polymeric structures.

The nomenclature used in the experiment includes the numbering corresponding to each quadrant (1–27); the manufacturer MTN® Montana Colors (MTN), Montana™ Cans (M); the aerosol type MTN 94 (94), Water-Based (WB), Nitro2G (N2G), Nitro Tarblack (T) and Hardcore (H); and the aerosol colour Red (R), Green (V), Blue (A), Purple (M), Black (N) and Silver (P).

2.2. Experimental Procedure

To determine the effectiveness of the ultra-freezing method for removing graffiti from railway vehicles, air at a cryogenic temperature was jetted onto the graffiti applied onto the COA1 test tube. First of all, the equipment was adapted by performing a bleed in the closed air cycle. A 5 mm-diameter throat nozzle was adapted to the end of the hose, with which the controlled ultra-cold air projection tests were carried out. During application, exposure times were controlled by opening and closing the valve at station 7 in Figure 2. Temperature was measured right before the bleeding point, inside the facility, and at the nozzle, to quantify the temperature loss (the reason why the hose was thermally insulated, as can be seen in Figure 1) and to know the exact projection temperature. Type-T thermocouples with 0.5 K of uncertainty were used. Pressure was measured upstream of the hose with absolute-pressure piezoresistive transducers, the range of measurement of the sensor was 0–6 bar, and the uncertainty had a non-linearity of 0.5%. Therefore, shots were guaranteed with temperature values close to $-80\text{ }^{\circ}\text{C}$, 3 bars of pressure, and 0.5 cm of projection distance, causing exposure times of 30", 1', 2', 4', 6' and 8' on the substrate. On aerosols, a single 8 min shot was administered for each colour, increasing the time (++) by a second shot on those that experienced greater sensitivity (Table 2).

Table 2. Control parameters for ultra-cold projection tests. Source: own elaboration.

Air Temperature	Jet Pressure	Exposure Time	Shot Distance
$-80\text{ }^{\circ}\text{C}$	3 bar	30"/1'/2'/4'/6'/8'/++	0.5 cm

Source: own elaboration, 2024.

2.3. Methods of Analysis and Recording of Results

The resistance of the support materials and graffiti to low temperatures was assessed by recording and analysing pre- and post-freezing tests. Analyses were performed with non-destructive and destructive contact measurement systems on the sample in order to assess the surface and underlying layers by microscopic means, as well as to evaluate changes in topography, adhesion and colourimetry of the materials involved.

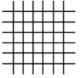
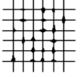
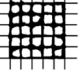
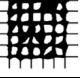
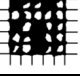
2.3.1. Analysis by Microscopy

Changes in the topography of the materials and layering were examined by microscopy. Surface analysis was carried out using a Dino Lite® AD4113ZT polarising microscope (Absolute Data Services Ltd., Hemel Hempstead, UK). Studies under ultraviolet (UV, 400 nm) and infrared (IR, 940 nm) illumination were made with a Dino Lite® AD413T-I2V (Absolute Data Services Ltd., Hemel Hempstead, UK).

2.3.2. Adhesion Analysis

The changes in spray adhesion were evaluated using a NEURTEK® NK2000® multi-blade hand-held grating cutter (Neurtek Instruments, Eibar, Spain) [62] Type 2a, according to the ISO 2409:2020 classification of test tool types [63] and standardised tape Tesa® 4024 PV 2 [64]. The results have been classified according to the categories stipulated by the standard (Table 3), by recording with Dino Lite® AD4113ZT at x50.

Table 3. Results classified according to cross-cut area effect.

Classification	Description	Cross-Cut Area Affected	Appearance
0	Clean cuts without detachment.	0%	
1	Small losses at intersections.	<5%	
2	Detachment at edges and intersections.	5–15%	
3	Loss of partial coating in strips. Total or partial absence in several squares.	15–35%	
4	Total separation of the stratum in some squares. Wide bands around the cuts.	35–65%	
5	Any loss in excess of that described in Classification 4.	>65%	-

Source: Data derived from ISO 2409:2020 [63] standard document.

2.3.3. Colourimetric Analysis

A colourimetric analysis makes it possible to record and evaluate changes in the colour and luminosity of the surface, which are conditions that are complementary to the loss of adhesion. The colourimetric alterations of the surfaces before and after treatment were evaluated according to UNE-EN 15886 [65]. The measurements were carried out with a Minolta® CM-2600d spectrophotometer (Konica Minolta, Inc., Tokyo, Japan) [66]. Data processing allowed the calculation of the total colour differences (ΔE^*) and standard deviation of the aerosols and the support measures.

3. Results

The data collected during the experimentation included microscopic analysis, colourimetric analysis, and adhesion test by lattice cutting to evaluate the resistance of the coatings. The use of a microscope with polarised light has allowed the surface characterisation

of the specimen, as well as the recording of alterations and applied tests. The most representative results of the experimental development are shown below.

3.1. Deep-Freezing Conditions Obtained

Due to the adaptation of the deep-freezing equipment for the bleeding cycle, a recording of the outlet temperature, surface temperature and pressure conditions was carried out. These values oscillate during the exposure time, recovering the cycle constants ($-80\text{ }^{\circ}\text{C}$, 3 bar) after each shot. The values recorded during the thermal resistance tests of the support (Table 4), as well as the exposure test of the aerosols with fixed and moving (oscillating and rotating) blasting of ultra-frozen air (Table 5), were collected by thermocouples connected to the control terminal. The outlet temperature suffers a minimum offset of $+5\text{ }^{\circ}\text{C}$ with respect to the surface temperature, the ratio of which increases with a greater distance of projection.

Table 4. Test of thermal resistance of the substrate. Cycle conditions: exposure times, temperature, pressure and throw distance. Source: own elaboration, 2023.

Code	Nozzle Temperature ($^{\circ}\text{C}$)	T Surface ($^{\circ}\text{C}$)	Pressure (bar)	Time	Distance (cm)
COA1	-85	-80	2.95	30"	0.5
COA1	-85	-80	2.95	1'	0.5
COA1	-85	-80	2.95	2'	0.5
COA1	-80	-75	2.95	4'	0.5
COA1	-80	-75	2.95	6'	0.5
COA1	-80	-75	2.95	8'	0.5

Table 5. Aerosol thermal resistance tests. Cycle conditions: temperature, pressure, exposure times and projection distance. Source: own elaboration, 2023.

Code	Nozzle Temperature ($^{\circ}\text{C}$)	T Surface ($^{\circ}\text{C}$)	Pressure (bar)	Time (min)	Distance (cm)
17_MTN_94_N	-83	-78	3.08	8	0.5
18_MTN_94_N					
19_MTN_WB_N	-86	-81	3.05	8	0.5
20_MTN_WB_N					
21_MTN_N2G_N	-83	-78	3.07	8	0.5
22_MTN_N2G_N					
23_MTN_T	-82	-77	3.07	8	0.5
24_MTN_T					
5_MTN_94_V	-83	-78	2.88	8	0.5
6_MTN_94_V					
7_MTN_WB_V	-84	-79	2.9	8	0.5
8_MTN_WB_V					
13_MTN_94_M	-84	-79	2.86	8	0.5
14_MTN_94_M					
15_MTN_WB_P	-83	-78	3	8	0.5
16_MTN_WB_P					
1_MTN_94_R	-82	-77	2.82	8	0.5
2_MTN_94_R					
3_MTN_W_R	-83	-78	2.85	8	0.5
4_MTN_WB_R					
9_MTN_94_A	-82	-77	2.92	8	0.5
10_MTN_94_A					
11_MTN_WB_A	-85	-80	2.94	8	0.5
12_MTN_WB_A					

25_MTN_HP	-85	-80	3.1	8	0.5
26_MTN_HP					
23_MTN_T	-80	-75	3	++	0.5
24_MTN_T					

3.2. Microscopy

After cold exposure of the original coatings on the substrate, the surface was examined with polarised light, ultraviolet light, and infrared microscopy in order to obtain information on lower strata such as preparations and intermediate layers. Fewer contaminant particles are visible deposited on the surface. The finishes retain their original appearance, regarding homogeneity and defects due to use. The microscopic documentation does not show any degradation or changes that would negatively affect the conservation of the support.

Relevant chromatic and topographic changes have been identified in the aerosols. In some cases, the surface has become rougher and stiffer, showing a slight stoning of the surface. This could be a physicochemical alteration that some polymers undergo in removal processes, causing a whitish appearance that alters the original perception of colour. The aerosols with which this alteration is most noticeable are MTN_WB_R, MTN_94_R, MTN_WB_M and M_T.

In the MTN_94_R, MTN_WB_R and MTN_WB_M aerosol samples, alterations can be seen in the topography, which is irregular, and there are particles that cause visible chromatic alterations. The texture is accentuated and white mottling is visible in the interstices of the material (Figures 5–7).

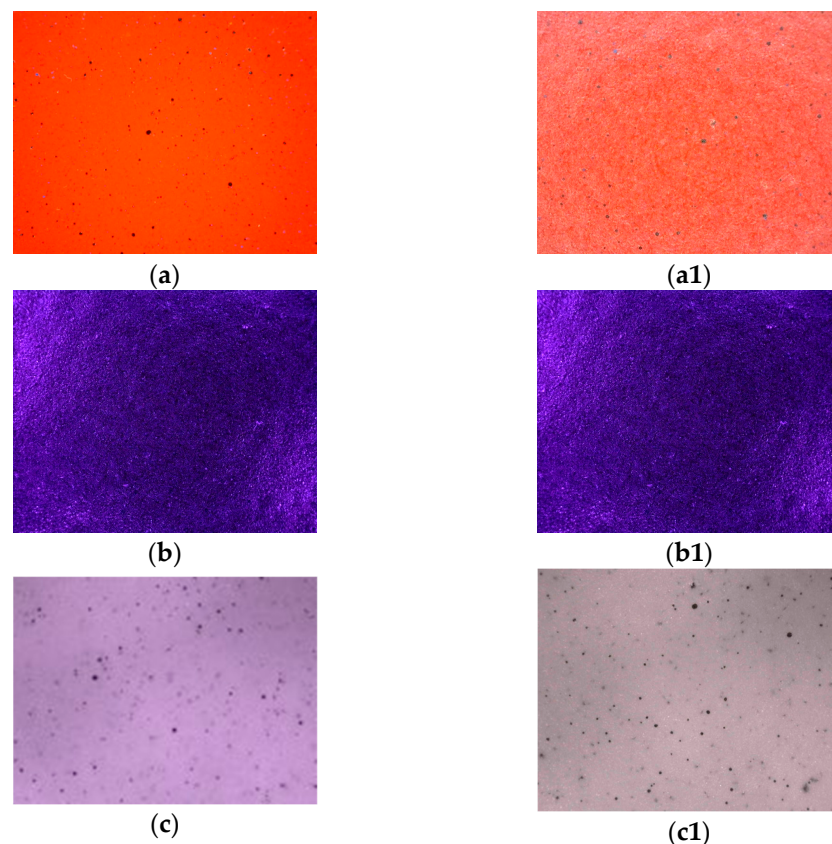


Figure 5. Microscopic examination of MTN_94_R x50 with Dino Lite® and Dino Lite® AD413T-I2V: (a–c) pre-treatment spray; (a1–c1) appearance after cold application. Source: own authorship, 2023.

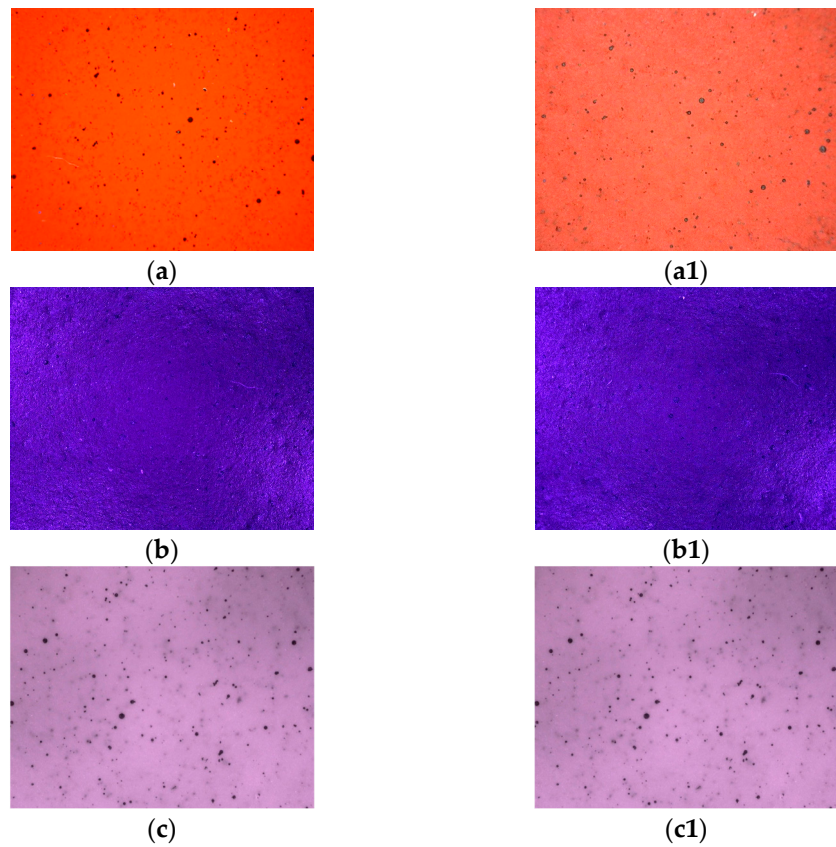


Figure 6. Microscopic examination of MTN_WB_R x50 with Dino Lite® AD4113ZT and Dino Lite® AD413T-I2V: (a–c) pre-treatment spray; (a1–c1) appearance after cold application. Source: own authorship, 2023.

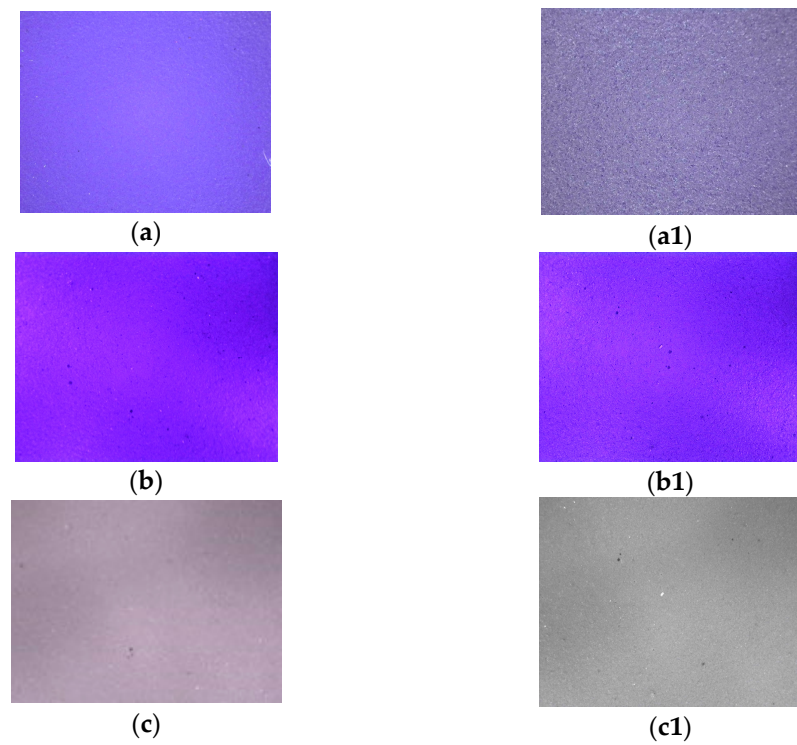


Figure 7. Microscopic examination of MTN_WB_M x50 with Dino Lite® AD4113ZT and Dino Lite® AD413T-I2V: (a–c) pre-treatment spray; (a1–c1) appearance after cold application. Source: own authorship, 2023.

The bitumen-based polymer M_T has a vitrified appearance with surface morphology showing more abrupt edges and conglomerates as a result of material shrinkage (Figure 8). The mottling caused by material contamination is reduced after cryogenic exposure. In the image taken with UV and IR light, more accentuation of the cavities caused by the aerosol application methodology was identified, as well as a more satin finish.

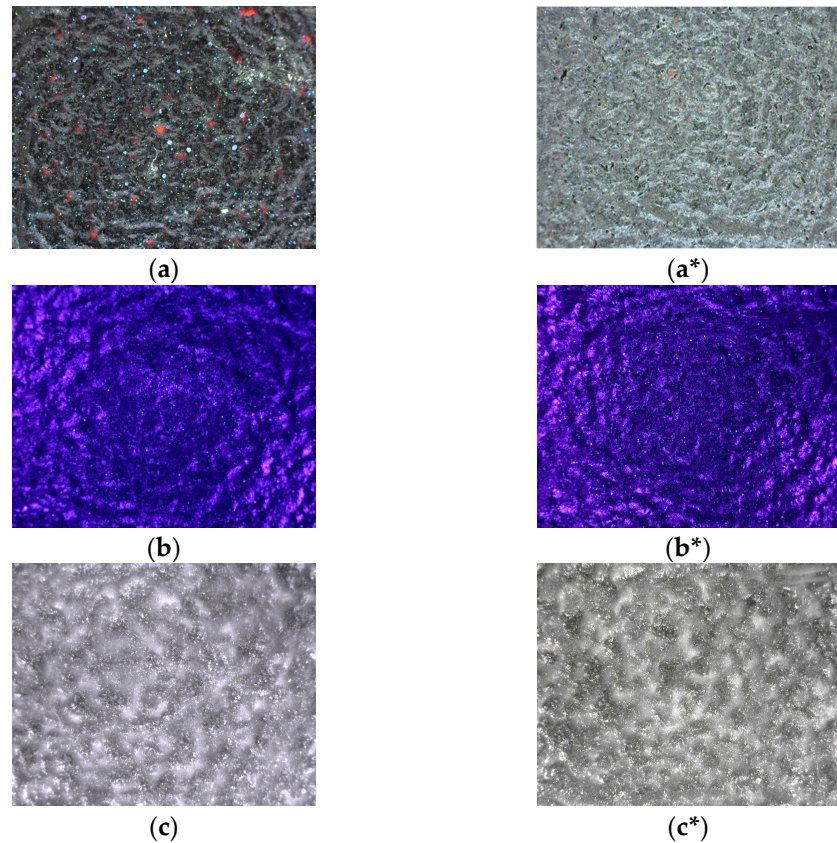


Figure 8. Microscopic examination of M_T x50 with Dino Lite® AD4113ZT and Dino Lite® AD413T-I2V: (a–c) pre-treatment spray; (a*–c*) appearance after cold application. Source: own authorship, 2023.

Keeping the conditions of pressure (3 bar), distance (0.5 cm) and temperature (-80°C) constant, the M_T aerosol was sprayed in areas with the highest roughness. During the spraying, the stratum peeled off. The incidence of air caused a thermal shock that induced the loss of adhesive forces binding the aerosol to the substrate. The consequences of the thermal effect are visible macroscopically (Figure 9) and the glassy nature of the fractured edges of the polymer can be observed (Figure 10).

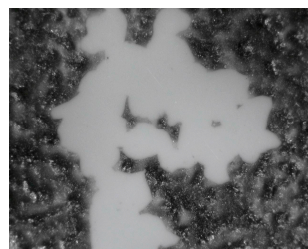


Figure 9. Fracture of the polymer. Zone 23_M_T. IR x50 with Dino Lite® AD413T-I2V. Source: own authorship, 2023.



Figure 10. Experimental test of the effect of cold on intercoat adhesion. Zone 23_M_T: (a,b). Source: own authorship, 2023.

3.3. Adhesion

The characterisation of adhesion by lattice cutting of the original coatings of the COA1 substrate indicates that it is a category 0 laminate (Table 6): the incisions caused by the equipment do not show flaking and are perfectly smooth. The effect of the cold (-75°C , 0.5 cm distance, 8 min) has produced a slight alteration in the adhesion, corresponding to category 1. Therefore, we perceive that it is a 1–2% effect (see Figure 11), as we observe in the interstices of the cut a slight flaking that causes a jagged effect. This could also indicate defects in the lattice-cut test method.



Figure 11. COA1 x50 grating cut with Dino Lite® AD4113ZT: (a) initial adhesion; (b) effect of cold. Source: own authorship, 2023.

Table 6. Adhesion test results by lattice cutting. Adhesion values before and after treatment. Source: own elaboration, 2023.

Code	Cutting Tool	Classification * (Before)	%	Classification (After)	%
COA1	2a	0	0%	1	<5%
MTN_94_N	2a	1	<5%	1	<5%
MTN_WB_N	2a	1	<5%	1	<5%
MTN_N2G_N	2a	2	5–15%	3	15–35%
M_T	2a	1	<5%	1	<5%
MTN_94_V	2a	2	5–15%	2	5–15%
MTN_WB_V	2a	1	<5%	1	<5%
MTN_94_M	2a	1	<5%	2	5–15%
MTN_WB_M	2a	1	<5%	1	<5%
MTN_94_R	2a	0	0%	0	0%
MTN_WB_R	2a	0	0%	0	0%
MTN_94_A	2a	1	<5%	1	<5%
MTN_WB_A	2a	1	<5%	1	<5%
MTN_HP	2a	0	0%	0	0%
M_T	2a	1	<5%	5	>65–100%

* Classification according to ISO 2409:2020 [63].

With regard to the changes in the adhesion of the aerosol-coated laminate to the substrate, the classification of the MTN_NN2G_N polymer without ultra-cold treatment corresponds to Classification 2. The affected area of the aerosol grid is 5–15%. After 8' of cryogenic blasting, there was an increase in the affected area, corresponding to a release rate of 15–35% (Classification 3), with no alteration in the characteristics of the substrate coating. The aerosol flaking extends along the edges in large bands, accompanied by losses affecting the area of the squares (see Figure 12). On the other hand, the MTN_94_M material responded with a noticeable loss of adhesion after application of a constant cryogenic temperature. The initial Classification (1) was altered with the effect of the cold, causing flaking in the incisions equal to 5%, corresponding to Category 2 (see Figure 13). The adhesion test carried out on the M_T aerosol after the application of ultra-cold air also shows a decrease in adhesion, increasing the percentage of loss to close to 5%. This results in the adhesion classification of the coating, whose category is between Type 1 and 2 (see Figure 14). However, by increasing the exposure time above 8' (+), 100% loss was achieved (Classification 5).



Figure 12. Lattice cut MTN_N2G_N x50 with Dino Lite® AD4113ZT: (a) initial adhesion; (b) effect of cold. Source: own authorship, 2023.



Figure 13. MTN_94_M x50 lattice cut with Dino Lite® AD4113ZT: (a) initial adhesion; (b) effect of cold. Source: Own authorship, 2023.



Figure 14. M_T x50 grating cut with Dino Lite® AD4113ZT: (a) initial adhesion; (b) effect of cold. Source: own authorship, 2023.

3.4. Colourimetry

An initial and final colourimetric evaluation was obtained to evaluate the effect of the cold on the limited areas of incidence of the ultracold air. According to guidelines used for practical interpretation of ΔE_{ab}^* , which measures the colour difference between two colour patches when viewed alongside each other, colour differences below 3 CIELab are

hardly perceptible, those between 3 and 6 are perceptible, and those above 6 represent significant colour differences [67]. The data obtained on the response to cold of the aerosols tested (see Figure 15) indicate that the MTN_WB_R (6.00) and MTN_94_R (4.59) colours have experienced the greatest changes in colour.

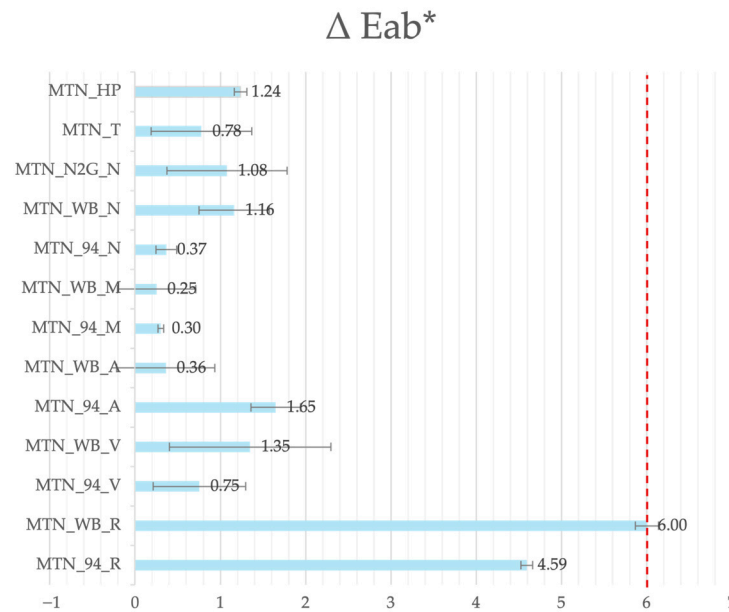


Figure 15. ΔE_{ab}^* aerosols tested, including standard deviation. Source: own elaboration, 2023.

In turn, on sample 23_M_T and in the analysis for the preservation of the physical–chemical qualities of the support, the colourimetric response of the CAO1 after the detachment of the aerosol was documented. Thus, a sampling of the clean area was carried out, comparing the original state of the support before and after the test (see Figure 16). Therefore, no significant colour differences were observed in the substrate, displaying a ΔE_{ab}^* of 3.26 CIELab units.

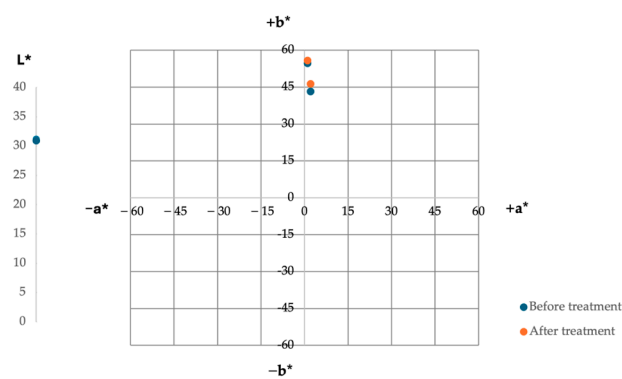


Figure 16. CIELAB diagram of the support for area 23_MTN_T. Source: own elaboration, 2023.

On the other hand, through the calculation of the colour difference caused on the coatings of the COA1 test piece (see Figure 17), we can validate the fact that the surface remains in good condition, without significant chromatic alterations.

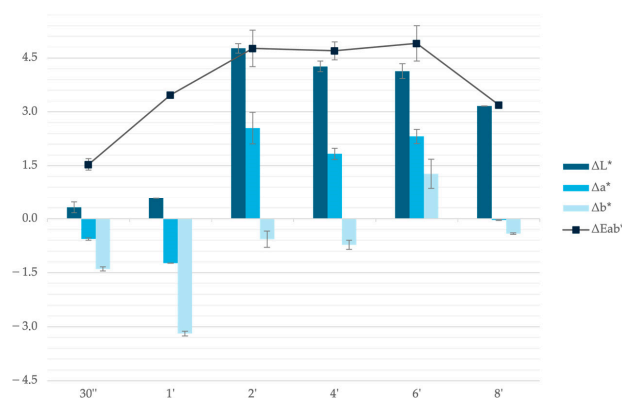


Figure 17. COA1 colourimetric study. Total colour difference (ΔE^*) including standard deviation. Source: own elaboration, 2023.

4. Discussion

Unwanted graffiti is a source of conflict in urban areas, especially in railway environments. It is a polarised issue that involves social, economic, political, and environmental issues in cities around the world. Cleaning graffiti from trains, tracks and stations is a challenge for local infrastructure maintenance companies. They recognise that they use inefficient and unsatisfactory cleaning methods, forcing trains to stop, disrupting timetables, and affecting passenger transport. The methods are also harmful to the operator's health and to the environment, and can be abrasive to the underlying materials and affect the vehicle's finish. In view of the number of drawbacks, we believe it is necessary to propose alternative solutions that are satisfactory and reduce the use of highly polluting substances.

Through the experimental procedures described and the results obtained in this study, we can advance information regarding the resistance to low temperatures of the support materials used in transport vehicles. In order to achieve a safe and efficient removal that does not alter the finish of the substrate, the thermal effect of the air jet has respected the safety ranges for the preservation of the appearance of the CAO1 coatings. Microscopy, adhesion and spectrophotometric studies do not indicate significant damage to the polymeric structure of the coating. On the other hand, the results obtained in the experimental tests on the spray paints suggest an improvement in the cleaning and graffiti-removal processes. The test has brought us closer to the safety ranges of the aerosols, finding certain degradations that could be aggravated with a greater incidence of cold or air pressure. The microscopic study showed alterations in the topography of the material. Adhesion tests by lattice cutting show that there has been a loss of aerosol-support cohesion after the application of constant cold. All materials displayed detachment levels under 35% (Classifications 1–3), except for the M_T aerosol, which experienced complete detachment (Classification 5). In this sense, the loss of adhesion of some layers confirms that a physicochemical failure occurs after the thermal *shock*. This may be due to various factors such as the type of binder, colouring substance, fillers, or other additives. Paints with modified alkyd–acrylic binder and modified polyurethane have lost adhesion and experienced colour changes. Bitumen-based paints were removed by cryogenic blasting. Data on colour difference (0.78) and loss of adhesion (0–5%) after 8' of ultra-cold blasting indicate that the material is very resistant to cold. However, it was detached from the substrate when blasting from different angles for a longer time, maintaining distance (0.5 cm), temperature (<-80 °C) and pressure (2.95–3 bar).

The study carried out with the adapted deep-freezing equipment allowed thermal-sensitivity tests to be carried out. As this is a cycle whose equilibrium depends on a closed air circuit, sufficient air extraction has been achieved to obtain results for the effect of cold with pressurised air for the elimination of aerosols. The adaptation of the inverse Brayton

cycle has exceeded the working temperature of dry-ice blasting with solid carbon dioxide ($-79\text{ }^{\circ}\text{C}$ at the outlet/ $-12\text{ }^{\circ}\text{C}$ at the surface) and liquid ($-18\text{ }^{\circ}\text{C}$ at the outlet/ $8\text{ }^{\circ}\text{C}$ at the surface), without altering the properties of the support, achieving the removal of the M_T aerosol with pressure ranges much lower than cryogenic ones (3 bar).

Analysis of the data obtained from the experimental tests showed that, in general, the aerosols are affected by low temperatures, showing changes in adhesion and colourimetry. The results suggest that the ultra-freezing method could be effective for the removal of graffiti from railway vehicles. Given the heterogeneous response to cold, determining the variables that interfere with detaching the aerosol will lead to improvements in future experimental studies by determining the percentage of responsibility for the independent and combined thermal and mechanical effect.

5. Conclusions

Tests on the use of the projection of ultra-cooled air for the removal of graffiti from railway vehicles have yielded significant results both for the degradation of the aerosols used in the graffiti and in the preservation of the vehicle's support materials. The preservation of these materials was confirmed by observing that they maintained their integrity without significant alterations in their adhesion, measuring variations of less than 5%, and in colourimetry, with ΔEab^* results above 6 CIE Lab units (4.91), which are deemed acceptable according to industry standards [67].

On the other hand, the degradation of the aerosols varied depending on the type of paint, showing noticeable changes in topography and adhesion. Bitumen-based paints, specifically MTN_T aerosol, stood out for their complete removal under specific conditions of pressure (3 bar), temperature ($<-80\text{ }^{\circ}\text{C}$), and increased exposure time, showing a 100% total loss of adhesion with prolonged treatment. In addition, significant changes were observed in the colourimetry and adhesion of the aerosols. The red colours, represented by the variants MTN_WB_R and MTN_94_R, experienced the largest colourimetric alterations, with differences of up to 6.00 and 4.59 in ΔEab^* , respectively.

The adhesion of certain aerosols decreased markedly, with MTN_N2G_N being a prominent case, which, after 8 min of exposure to cold air, intensified its adhesion loss from a range of 5–15% to 15–35%. This demonstrates that ultra-cooled-air blasting is a promising and viable method for the removal of graffiti on rail vehicles, achieving effective removal of certain paints without compromising the integrity of the supporting materials. These results underline the potential of this technique as a sustainable and environmentally friendly solution for graffiti management in urban environments, paving the way towards the optimisation and practical application of this innovative cleaning method.

Author Contributions: Conceptualization, V.S.-C. and A.V.-B.; methodology, V.S.-C. and A.V.-B.; investigation, A.V.-B. and V.S.-C.; resources, A.V.-B. and V.S.-C.; writing—original draft preparation, A.V.-B., V.S.-C., J.A.L.-C. and V.D.-R.; writing—review and editing, A.V.-B., V.S.-C., P.B.-R., J.A.L.-C., V.D.-R. and M.S.-P.; supervision, V.S.-C. All authors have read and agreed to the published version of the manuscript.

Funding: The authors would like to acknowledge the support received for this research from the Vice-Rectorate for Research of the Polytechnic University of Valencia (PAID-11-22), grant number PID2022-139433OB-I00, as well as the collaboration with Istobal S.A., facilitated by the ISTOBAL Chair of the Polytechnic University of Valencia (UPV). In addition, the authors would like to express their gratitude to CEICE-GVA and its grant Programme for Doctoral Studies (CIACIF/2021/404), funded by the European Union.

Institutional Review Board Statement: Not applicable.

Informed Consent Statement: Not applicable.

Data Availability Statement: The raw data supporting the conclusions of this article will be made available by the authors on request.

Conflicts of Interest: The authors declare no conflicts of interest.

Abbreviations

The following abbreviations are used in this manuscript:

CC	Climatic chamber
EC	Electric compressor
GWP	Global warming potential
IC	Intercooler
ODP	Ozone depletion potential
RBC	Reverse Brayton cycle
REG	Regenerator
T	Turbine
TCC	Turbocharger compressor

References

1. Sánchez, M. Acercamiento a la evolución histórica y tecnológica de los materiales pictóricos. In *ARTE URBANO. Conservación y Restauración de Intervenciones Contemporáneas*. Ge-IIC: Madrid, Spain, 2016; Volume 10, pp. 146–159. <https://doi.org/10.37558/gec.v10i0.408>
2. Halsey, M.; Young, A. “Our desires are ungovernable” Writing graffiti in urban space. *Theor. Criminol.* **2006**, *10*, 275–306. <https://doi.org/10.1177/1362480606065908>.
3. Thompson, K.; Offler, N.; Hirsch, L.; Every, D.; Thomas, M.J.; Dawson, D. From broken windows to a renovated research agenda: A review of the literature on vandalism and graffiti in the rail industry. *Transp. Res. Part A Policy Pract.* **2012**, *46*, 1280–1290. <https://doi.org/10.1016/J.TRA.2012.04.002>.
4. Teng, H.H.; Puli, A.; Qi, Y.G. Identification of Influencing Factors of Graffiti Occurrence at Nevada State Highway Bridges and Soundwalls. *J. Infrastruct. Syst.* **2017**, *23*, 05017003. [https://doi.org/10.1061/\(ASCE\)IS.1943-555X.0000368](https://doi.org/10.1061/(ASCE)IS.1943-555X.0000368).
5. Moura, A.R.; Flores-Colen, I.; de Brito, J. Analysis of graffiti removal techniques and anti-graffiti products for porous materials. In *Proceedings of the Hydrophobe VII—7th International Conference on Water Repellent Treatment and Protective Surface Technology for Building Materials*; Lisboa, 2014. <https://doi.org/10.13140/RG.2.1.4502.6640>.
6. Roviello, V.; Gilhen-Baker, M.; Roviello, G.N. Graffiti Paint on Urban Trees: A Review of Removal Procedures and Ecological and Human Health Considerations. *Sustainability* **2023**, *15*, 4022. <https://doi.org/10.3390/su15054022>.
7. Kelling, G.L.; Wilson, J.Q. Broken Windows. *Atl. Mon.* **1982**, *249*, 29–38. Available online: <http://www.theatlantic.com/magazine/archive/1982/03/broken-windows/304465/1> (accessed on 20 February 2024).
8. Haworth, B.; Bruce, E.; Iveson, K. Spatio-temporal analysis of graffiti occurrence in an inner-city urban environment. *Appl. Geogr.* **2013**, *38*, 53–63. <https://doi.org/10.1016/J.APGEOG.2012.10.002>.
9. Fernandes, C.; Batel, S. The right to stay: Exploring graffiti and street art as political representations against touristification in Lisbon. *Pap. Soc. Represent.* **2023**, *32*, 2.1–2.26. Available online: <https://psr.iscte-iul.pt/index.php/PSR/article/view/678> (accessed on 19 February 2024).
10. Huntington, D. Sustainable Graffiti Management Solutions for Public Areas. *SAUC-Str. Art. Urban Creat.* **2018**, *4*, 46–74.
11. McAuliffe, C. Legal Walls and Professional Paths: The Mobilities of Graffiti Writers in Sydney. *Urban Stud.* **2013**, *50*, 518–537. <https://doi.org/10.1177/0042098012468894>.
12. Sanmartín, P.; Bosch-Roig, P. Biocleaning to Remove Graffiti: A Real Possibility? Advances towards a Complete Protocol of Action. *Coatings* **2019**, *9*, 104. <https://doi.org/10.3390/coatings9020104>.
13. Graffiti Costs UK Over £100 Million Every Year. Marketers Media Newsroom. Available online: <https://news.marketersmedia.com/graffiti-costs-uk-over-100-million-every-year/88901842> (accessed on 6 February 2024).
14. Medina, F. El Coste de Limpiar los Grafitis se Dispara en Madrid: Más de 10.000 Euros al Día. *El Mundo*. Available online: <https://www.elmundo.es/madrid/2019/09/01/5d6a92f6c6c83ee4c8b4571.html> (accessed on 13 February 2024).
15. Killen, A.; Coxon, S.; Napper, R. A Review of the Literature on Mitigation Strategies for Vandalism in Rail Environments. In *Proceedings of the 39th Australasian Transport Research Forum (ATRF)*, Auckland, New Zealand, 27–29 November 2017.
16. Havârneanu, G.M. Behavioral and organizational interventions to prevent trespass and graffiti vandalism on railway property. *Proc. Inst. Mech. Eng. F J. Rail Rapid Transit* **2017**, *231*, 1078–1087. <https://doi.org/10.1177/0954409716675004>.
17. Uzzell, D.; Brown, J. Conceptual Progress in Understanding Fear of Crime in Railway Stations. *Psicologia* **2007**, *21*, 119–137.
18. Enever, P. Cutting graffiti costs through Queensland Rail prevention and management. In *AusRAIL PLUS 2013, Driving the Costs out of Rail*; Canberra, ACT, Australia, 26–28 November 2013.
19. Rodríguez, J. Entre 15 y 25 Millones de Euros Anuales: El Coste de los Grafitis en los Trenes de Renfe. *El Confidencial*. Available online: https://www.elconfidencial.com/espana/2019-02-21/juicios-grafiteros-trenes-renfe-aumentaron_1839774/ (accessed on 6 February 2024).

20. Renfe Gasta 25 Millones de Euros al Año en Evitar y Limpiar Grafitis en Sus Trenes. Europa Press. Available online: <https://www.europapress.es/economia/noticia-renfe-gasta-25-millones-euros-ano-evitar-limpiar-grafitis-trenes-20181116140347.html> (accessed on 6 February 2024).
21. Rovira, M. Los Grafitis en los Trenes en Cataluña Cuestan 6.5 Millones de Euros a Renfe. EL PAÍS. Available online: <https://elpais.com/espana/catalunya/2021-01-19/los-grafitis-en-los-trenes-cuestan-65-millones-de-euros-a-renfe.html> (accessed on 18 July 2023).
22. Morales, E. Renfe Adjudica un Macrocontrato de Más de 400 Millones Para Limpiar Estaciones y Grafitis. The Objective Media S.L. Available online: <https://theobjective.com/economia/2023-01-07/renfe-contrato-millones-grafitis-celse-acciona/> (accessed on 18 July 2023).
23. Removing Graffiti from Trains Cost SNCB €6 Million in 2020. The Brussels Times. Available online: <https://www.brusselstimes.com/177167/removing-graffiti-from-trains-cost-sncb-e6-million-in-2020> (accessed on 6 February 2024).
24. Wighton, D. Graffiti en Trenes: Cómo Aborda ALEMANIA su Problema de 38 Millones de Euros. The Local de. Available online: https://www-thelocal-de.translate.goog/20190510/train-graffiti-how-germany-is-tackling-its-38-million-problem?_x_tr_sl=en&_x_tr_tl=es&_x_tr_hl=es&_x_tr_pto=sc (accessed on 6 February 2024).
25. Jardim, V. Graffiti Criminals Costing \$30 m, Delaying Commuters—And Risking Death. 9 News. Available online: <https://www.9news.com.au/national/graffiti-criminals-sydney-trains-cost-delays-death-and-injuries/849054e6-9287-45ef-b78f-f6985130df56> (accessed on 6 February 2024).
26. Marcin, G.; Paweł, K. Effectiveness of Anti-Graffiti Coatings used in Rolling Stock. *Terotechnology XI Mater. Res. Forum LLC Mater. Res. Proc.* **2020**, *17*, 233–239. <https://doi.org/10.21741/9781644901038-34>.
27. TeleMadrid. Así se Limpian los Grafitis de los Trenes de Cercanías de Madrid. Available online: <https://www.telemadrid.es/programas/telenoticias-1/limpian-grafitis-cuestan-RENFE-millones-2-2097110309--20190221030903.html> (accessed on 6 February 2024).
28. Anundi, H.; Langworth, S.; Johanson, G.; Lind, M.-L.; Åkesson, B.; Friis, L.; Itkes, N.; Soderman, E.; Jönsson, B.A.G.; Edling, C. Air and biological monitoring of solvent exposure during graffiti removal. *Int. Arch. Occup. Environ. Health* **2000**, *73*, 561–569.
29. Langworth, S.; Anundi, H.; Friis, L.; Johanson, G.; Lind, M.-L.; Söderman, E.; Åkesson, B.A. Acute health effects common during graffiti removal. *Int. Arch. Occup. Environ. Health* **2001**, *74*, 213–218.
30. Instituto Nacional de Seguridad y Salud en el Trabajo. ICSC 0360-HIDRÓXIDO DE SODIO. 2018. Available online: https://www.ilo.org/dyn/icsc/showcard.display?p_version=2&p_card_id=0360&p_lang=es (accessed on 28 February 2024).
31. Teng, H.; Puli, A.; Kutela, B.; Ni, Y.; Hu, B. Cost and Benefit Evaluation of Graffiti Countermeasures on the Nevada Highways. *J. Transp. Technol.* **2016**, *6*, 360–377. <https://doi.org/10.4236/JTTS.2016.65031>.
32. García García, M.; González Arrieta, M.A.; Rodríguez González, S.; Márquez-Sánchez, S.; Da Silva Ramos, C.F. Graffiti Identification System Using Low-Cost Sensors. *Int. J. Interact. Multimed. Artif. Intell.* **2023**, *in press*. <https://doi.org/10.9781/IJIMAI.2023.05.001>.
33. Willcocks, M.; Malpass, M.; Toyman, G. D2.1 Graffiti Vandalism in Public Areas and Transport Report and Categorisation Model. 2015. Available online: <http://project.graffolution.eu> (accessed on 19 February 2024).
34. Rossi, S.; Fedel, M.; Petrolli, S.; Deflorian, F. Behaviour of different removers on permanent anti-graffiti organic coatings. *J. Build. Eng.* **2016**, *5*, 104–113. <https://doi.org/10.1016/J.JOBE.2015.12.004>.
35. Amrutkar, S.; More, A.; Mestry, S.; Mhaske, S.T. Recent developments in the anti-graffiti coatings: An attentive review. *J. Coat. Technol. Res.* **2022**, *19*, 717–739. <https://doi.org/10.1007/s11998-021-00580-z>.
36. Rossi, S.; Fedel, M.; Petrolli, S.; Deflorian, F. Characterization of the Anti-Graffiti Properties of Powder Organic Coatings Applied in Train Field. *Coatings* **2017**, *7*, 67. <https://doi.org/10.3390/coatings7050067>.
37. Milescu, R.A.; Farmer, T.J.; Sherwood, J.; McElroy, C.R.; Clark, J.H. Cyrene™, a Sustainable Solution for Graffiti Paint Removal. *Sustain. Chem.* **2023**, *4*, 154–170. <https://doi.org/10.3390/suschem4020012>.
38. Quann, J. Irish Rail Looking at Innovative Ways to Remove Graffiti. News Talk. Available online: <https://www.newstalk.com/news/irish-rail-looking-at-innovate-ways-to-remove-graffiti-1163975> (accessed on 6 February 2024).
39. Renfe. “¿Cuánto Tiempo Crees Que Lleva Limpiar un Tren de Grafitis? #LaObraMásCara”. Available online: <https://twitter.com/renfe/status/1101421890835566592> (accessed on 6 February 2024).
40. Esto nos Cuestan los Grafitis: 6.5 Millones en 2020 Para Limpiar Pintadas en Rodalies. Metròpoli Abierta-El Español. Available online: https://metropoliabierta.elespanol.com/informacion-municipal/20210119/esto-nos-cuestan-los-grafitis-millones-en-para-limpiar-pintadas-rodalies/552444952_0.html (accessed on 6 February 2024).
41. Vega, A.; Santamarina, V.; Colomina, A.; Carabal, M.A. Cryogenics as an advanced method of cleaning cultural heritage. Challenges and solutions. *Sustainability* **2021**, *13*, 1052.
42. Kohli, R. Applications of dry vapor steam cleaning technique for removal of surface contaminants. In *Developments in Surface Contamination and Cleaning: Applications of Cleaning Techniques*. Elsevier: Amsterdam, The Netherlands, 2018; Volume 11, pp. 681–702. <https://doi.org/10.1016/B978-0-12-815577-6.00017-7>.
43. Kohli, R. Applications of Solid Carbon Dioxide (Dry Ice) Pellet Blasting for Removal of Surface Contaminants. In *Developments in Surface Contamination and Cleaning: Applications of Cleaning Techniques*. Elsevier: Amsterdam, The Netherlands, 2019; Volume 11, pp. 117–169. <https://doi.org/10.1016/B978-0-12-815577-6.00004-9>.
44. Spur, G.; Uhlmann, E.; Elbing, F. Dry-ice blasting for cleaning: Process, optimization and application. *Wear* **1999**, *233*, 402–411. Available online: www.elsevier.com/locate/wear (accessed on 30 January 2024).

45. Dzido, A.; Krawczyk, P. Abrasive Technologies with Dry Ice as a Blasting Medium. *Energies* **2023**, *16*, 1014. <https://doi.org/10.3390/EN16031014>.
46. Máša, V.; Hornák, D.; Petrilák, D. Industrial use of dry ice blasting in surface cleaning. *J. Clean. Prod.* **2021**, *329*. <https://doi.org/10.1016/j.jclepro.2021.129630>.
47. Krier, P.; White, B.T.; Ferriday, P.; Watson, M.; Buckley-Johnstone, L.; Lewis, R.; Lanigan, J.L. Vehicle-based cryogenic rail cleaning: An alternative solution to “leaves on the line”. *Proc. Inst. Civ. Eng. Civ. Eng.* **2021**, *174*, 176–182. <https://doi.org/10.1680/jcien.21.00105>.
48. Mašková, L.; Smolík, J.; Vávrová, P.; Neoralová, J.; Součková, M.; Novotná, D.; Jandová, V.; Ondráček, J.; Ondráčková, L.; Křížová, T.; et al. Carbon dioxide snow cleaning of paper. *Herit. Sci.* **2021**, *9*, 145. <https://doi.org/10.1186/S40494-021-00622-0>.
49. Onofre, A.; Godina, R.; Carvalho, H.; Catarino, I. Eco-innovation in the cleaning process: An application of dry ice blasting in automotive painting industry. *J. Clean Prod.* **2020**, *272*, 122987. <https://doi.org/10.1016/j.jclepro.2020.122987>.
50. Millman, L.R.; Giancaspro, J.W. Environmental Evaluation of Abrasive Blasting with Sand, Water, and Dry Ice. *Int. J. Arch. Eng. Constr.* **2012**, *1*, 174–182. <https://doi.org/10.7492/ijaec.2012.019>.
51. Suárez Koch, J.J. Estudio de Prefactibilidad Para La Instalación de Un Servicio de Limpieza Criogénica Con Hielo Seco Para El Sector de Generación de Energía Eléctrica. Universidad de Lima. 2020. Available online: https://repositorio.ulima.edu.pe/bitstream/handle/20.500.12724/11574/Su%c3%a1rez_Koch_Jimena_Josceline.pdf?sequence=1&isAllowed=y (accessed on 29 July 2022).
52. Desantes, J.M.; Benajes, J.V.; Broatch, J.A.; Galindo, L.J.; Serrano, C.J.R.; Olmeda, G.P.C.; Dolz, R.V.; Fernandez, B.M. ES2747856 (A1). Espacenet. Available online: https://lp.espacenet.com/publicationDetails/biblio?DB=lp.espacenet.com&II=0&ND=3&adjacent=true&locale=es_LP&FT=D&date=20200311&CC=ES&NR=2747856A1&KC=A1 (accessed on 27 October 2022).
53. Desantes, J.M.; Benajes, J.V.; Broatch, J.A.; Galindo, L.J.; Serrano, C.J.R.; Olmeda, G.P.C.; Dolz, R.V.; Fernandez, B.M. WO2021123484 (A1). Espacenet. Available online: https://lp.espacenet.com/publicationDetails/originalDocument?FT=D&date=20210624&DB=lp.espacenet.com&locale=es_LP&CC=WO&NR=2021123469A1&KC=A1&ND=4 (accessed on 11 April 2024).
54. Serrano, J.R.; Dolz, V.; Ponce-Mora, A.; López-Carrillo, J.A. Experimental Assessment of a Reverse Brayton Cycle Based on Automotive Turbochargers and E-Chargers for Cryogenic Applications. *J. Eng. Gas Turbines Power* **2023**, *145*, 021029. <https://doi.org/10.1115/1.4055580>.
55. Marazioti, V.; Douvas, A.M.; Katsaros, F.; Koralli, P.; Chochos, C.; Gregoriou, V.G.; Boyatzis, S.; Facorellis, Y. Chemical characterisation of artists’ spray-paints: A diagnostic tool for urban art conservation. *Spectrochim. Acta A Mol. Biomol. Spectrosc.* **2023**, *291*, 122375. <https://doi.org/10.1016/J.SAA.2023.122375>.
56. Pellis, G.; Bertasa, M.; Ricci, C.; Scarcella, A.; Croveri, P.; Poli, T.; Scaroni, D. A multi-analytical approach for precise identification of alkyd spray paints and for a better understanding of their ageing behaviour in graffiti and urban artworks. *J. Anal. Appl. Pyrolysis* **2022**, *165*, 105576. <https://doi.org/10.1016/J.JAAP.2022.105576>.
57. Montana Colors, S.L. MTN 94. 2023. Available online: https://www.montanacolors.com/downloads/TDS_MTN_94_EN_23.pdf (accessed on 23 February 2024).
58. Montana Colors, S.L. Hardcore. 2020. Available online: https://www.montanacolors.com/downloads/TDS_MTN_Hardcore_EN.pdf (accessed on 23 February 2024).
59. Montana Colors, S.L. WATER BASED. 2020. Available online: https://www.montanacolors.com/downloads/TDS_MTN_Water-Based_400_EN.pdf (accessed on 23 February 2024).
60. Montana-Cans. MONTANA TARBLACK 600 ML. Available online: www.montana-cans.com/en/spray-cans/montana-spray-paint/black-50ml-600ml-graffiti-paint/montana-tarblack-600ml (accessed on 16 February 2024).
61. Montana Colors, S.L. Nitro 2G Negro. Available online: https://www.montanacolors.com/downloads/TDS_MTN_Nitro%202G_ES.pdf (accessed on 23 February 2024).
62. Neurtek Instruments. Corte Enrejado. Ensayo de Adherencia. 2023. Available online: https://www.neurtek.com/descargas/neurtek_corte_enrejado_es.pdf (accessed on 11 April 2024).
63. ISO 2409:2020; Paints and Varnishes—Cross-Cut Test. International Organization for Standardization: Geneva, Switzerland, 2020. Available online: <https://www.iso.org/standard/76041.html> (accessed on 18 July 2023).
64. Tesa®. Tesa® 4024. Poliiolefina High Tack. 2024. Available online: <https://www.tesa.com/es-es/industria/tesa-4024-poliiolefina-high-tack.html> (accessed on 11 April 2024).
65. AENOR. UNE-EN 15886 Conservación del Patrimonio Cultural. Métodos de Ensayo. Medición del Color de Superficies. 2010. Available online: www.aenor.es (accessed on 23 February 2024).
66. Konica Minolta, Inc. Espectrofotómetro CM-2600d/2500d; 2014. Available online: https://www.konicaminolta.com/instruments/download/instruction_manual/color/pdf/cm-2600d-2500d_instruction_spa.pdf (accessed on 11 April 2024).
67. Hardeberg, J.Y. *Acquisition and Reproduction of Color Images: Colorimetric and Multispectral*; Dissertation.com: Irvine, CA, USA, 2001.

Disclaimer/Publisher’s Note: The statements, opinions and data contained in all publications are solely those of the individual author(s) and contributor(s) and not of MDPI and/or the editor(s). MDPI and/or the editor(s) disclaim responsibility for any injury to people or property resulting from any ideas, methods, instructions or products referred to in the content.